



HAL
open science

Experimental study of the impact of alcohols on the oxidation stability of a surrogate jet-fuel

Ryma Benrabah, Zaki El Sayah, Minh Duy Le, Yvonne Anak Derrick Warren, Pierre-Alexandre Glaude, René Fournet, Baptiste Sirjean

► **To cite this version:**

Ryma Benrabah, Zaki El Sayah, Minh Duy Le, Yvonne Anak Derrick Warren, Pierre-Alexandre Glaude, et al.. Experimental study of the impact of alcohols on the oxidation stability of a surrogate jet-fuel. *Fuel*, 2024, 361, pp.130750. 10.1016/j.fuel.2023.130750 . hal-04403806

HAL Id: hal-04403806

<https://hal.science/hal-04403806>

Submitted on 18 Jan 2024

HAL is a multi-disciplinary open access archive for the deposit and dissemination of scientific research documents, whether they are published or not. The documents may come from teaching and research institutions in France or abroad, or from public or private research centers.

L'archive ouverte pluridisciplinaire **HAL**, est destinée au dépôt et à la diffusion de documents scientifiques de niveau recherche, publiés ou non, émanant des établissements d'enseignement et de recherche français ou étrangers, des laboratoires publics ou privés.

Experimental study of the impact of alcohols on the oxidation stability of a surrogate jet-fuel

Ryma Benrabah¹, Zaki El Sayah¹, Minh Duy Le¹, Yvonne Anak Derrick Warren¹, Pierre-Alexandre
Glaude¹, René Fournet¹, Baptiste Sirjean^{1,*}

¹ *Université de Lorraine, CNRS, LRGP, F-54000 Nancy, FR.*

ABSTRACT

The addition of biofuel in jet fuels can be seen as a promising answer to reduce the carbon footprint of the aviation transport sector. In this work, the impact of the addition of alcohols on the oxidation stability of a jet fuel surrogate was investigated. Different chemical structures of bioalcohols were considered and blended with *n*-decane used as the surrogate. The thermal oxidation stability of the mixtures was measured in a standard PetroOxy apparatus, which measures an induction period (IP). In addition to this global indicator of the fuel thermal stability, we quantified the total hydroperoxide concentration at the end of the test by iodometric titration. The influence of the length of the carbon chain in alcohols (1-butanol to 1-decanol) and the isomeric structure of butanols on the IPs of pure *n*-decane have been quantified. We show that the addition of a low percentage by volume of alcohols in the fuel increases its oxidation stability. This effect is non-linear, and the IP value increases with the volume percentage of alcohol in the fuel up to 10%. Beyond this value, a decrease in the stability of the mixture is observed. The influence of the length of the carbon chain is shown to be negligible. In contrast, the structure of butanol isomers strongly impacts the stabilization efficiency of the alcohol in the fuel. Conclusions on the fundamental chemical mechanism are drawn from *ab initio*

* Corresponding author (Baptiste Sirjean)

Baptiste.sirjean@univ-lorraine.fr

21 calculations and highlight the central role of the low bond dissociation energy of the H-atoms linked
22 to the carbon atom bearing the OH group in the liquid phase and the fate of the formed radical which
23 ultimately yields HO₂ and an aldehyde upon its reaction with O₂. This mechanism is specific to linear
24 alcohols and differs from the classic mechanism of autooxidation of alkanes.

25 **KEYWORDS:** autooxidation, *n*-decane, alcohol biofuels, jet-fuel, PetroOxy, *ab initio* calculations

26

27

28 **HIGHLIGHTS**

- 29 • Pure linear alcohols are found to have lower oxidation stability than *n*-decane
- 30 • The addition of alcohols to *n*-decane (1 to 20 vol.%) has an antioxidant effect
- 31 • The increase in oxidation stability is non-linear with the quantity of alcohol added
- 32 • Labile alcohol αH-atoms makes alcohols less stable and give them an antioxidant effect in
33 mixtures
- 34 • Alcohol peroxy radical yields an aldehyde + HO₂ rather than a hydroperoxide by H-abstractions

35

36 **INTRODUCTION**

37 New environmental regulations for the reduction of the carbon footprint of the aviation sector
38 encourage the use of sustainable biofuels since alternative power sources such as hydrogen and
39 batteries are not short- and medium-term solutions [1-4]. One challenge associated with the use of
40 “drop-in” biofuels, i.e., which can be used in current jet engines and logistic technologies, is that the
41 aviation jet fuel serves both as a coolant and an energy carrier. Therefore, the fuel is submitted to
42 high temperatures in aircraft as it circulate through the aircraft systems (hydraulic, lubrication,
43 combustor, etc.) to absorb excess heat. Since the fuel is in contact with oxygen from air throughout

44 all its chain of use, this high-temperature condition favors its kinetics of oxidation and its resistance
45 to this phenomenon is called thermal oxidation stability [5-9].

46 In the literature, experimental stability measurements based on deposit formation are referred to as
47 'thermal stability' while the measure of the ability to be oxidized is referred to as 'oxidative stability'
48 [10]. The adverse effects of liquid fuel oxidation (also called autoxidation) are well established and
49 lead to changes in its chemical composition, which ultimately yields the formation of gum and
50 deposits that affect crucial engine parts such as injectors, filters and pumps. The fundamental origin
51 of this autoxidation process comes from the presence of dissolved oxygen in the fuel and the chain
52 radical mechanisms that it allows. Nowadays, the understanding of this phenomenon is well known
53 for hydrocarbon fuels (RH) and involves an initiation step yielding alkyl radicals R• that will react with
54 O₂ and form peroxy radicals (ROO•). The main consumption pathways of ROO• is either the H-atom
55 abstraction from RH or its self-reaction through the Russell mechanism, yielding alcohols, ketones (or
56 aldehydes) and alkoxy radicals (RO•)[11-15]:



62 The kinetics of autoxidation of hydrocarbons can be inhibited by antioxidants or by lowering the
63 quantity of dissolved oxygen, or can be promoted by heteroatomic compounds or metal traces [10,
64 12, 16-18]. The effects of the addition of oxygenated molecules, such as those encountered in
65 biofuels, on the oxidation stability of hydrocarbons remain poorly understood and difficult to predict
66 depending on the nature of the oxygenated molecules [19]. As for the oxidation kinetics of pure
67 biofuels, it remains almost unexplored, except for biodiesel molecules.

68 Biodiesels are fatty acid mono-alkyl esters and the most used worldwide is the fatty acid methyl ester
69 (FAME) of animal or vegetable oil. In the literature, there are several reviews that deal with the
70 oxidation stability of biodiesels [20-22] and there is a consensus that their main drawback is their
71 poor resistance to oxidation because of the presence of unsaturated bonds in their chemical
72 structures. Nowadays, biodiesels are used in blends with conventional diesel fuels, up to 7% in most
73 cases, and the poor oxidation stability of FAME largely limits their use in larger quantities [20]. The
74 addition of 10% (v/v) of rapeseed FAME to diesel reduces its Induction Period (IP, quantitative
75 measure of oxidation stability in a standardized PetroOxy apparatus) by a factor 2.6 at 403 K [23].
76 The same research group found that the addition of the same proportion of methyl oleate to *n*-
77 dodecane reduced its induction period by a factor of 20 at 403 K [24]. These authors also
78 demonstrated that the IP of a pure fuel (diesel, jet fuel or *n*-dodecane) decreases nonlinearly with
79 the proportion of FAME added, from the higher value of IP for pure hydrocarbon fuel to the lowest
80 value of IP for the pure FAME considered [23, 24].

81 Similar studies on the oxidation stability of other families of potential biofuels, such as ethers, ketone
82 and alcohols, pure or blended with conventional fuels, are still scarce. Ethers studies are mostly
83 oxidation kinetic works in the liquid phase with and without antioxidants [25, 26]. In a previous
84 study, we showed that the addition of diethyl ether decreased the oxidation stability of *n*-decane,
85 which was acted as a surrogate jet-fuel [19]. The IP of pure *n*-decane was found to decrease
86 nonlinearly with the proportion of DEE added, from 1 to 20 % (v/v). At 413 K, the IP of a 80% *n*-
87 decane / 20% DEE mixture was decreased by about 30% compared to *n*-decane.

88 The studies on the oxidation stability of alcohols are focused on ethanol, and more particularly on
89 the consequences of its addition in gasoline, and the liquid blends oxidation, on standard EN and
90 ASTM tests [27-30]. Interestingly, D'Ornellas [28] showed that the addition of 13 to 25% (v/v) of
91 ethanol to gasoline leads to a lower storage stability in the gum formation test but a higher stability
92 for the change of color and the formation of insoluble tests. Recently, Auzani et al. [31] studied the

93 effect of ethanol addition on the IP of real and surrogates kerosene and showed, in PetroOxy
94 experiments, that ethanol addition (25 to 75%) decreases the oxidation stability of real kerosene but
95 increases that of surrogates. These differences remain difficult to interpret. In reference [19] we
96 demonstrated that the addition of small amounts of *n*-butanol dramatically increased the thermal
97 oxidation stability of *n*-decane with IPs increased by a factor of 6 at 413 K. This antioxidant effect
98 with regard to the PetroOxy test is surprising as all other biofuel families led to lower oxidation
99 stabilities and that the IP of pure *n*-butanol is lower to that of *n*-decane.

100 The present paper aims to determine the oxidation stability of pure alcohols and explore and
101 demonstrate their effects on the thermal oxidation stability of a jet-fuel surrogate, as a function of
102 their chemical structures and proportions. We will focus on the oxidation stability of a conventional
103 fuel surrogate, *n*-decane, which can be used as a jet surrogate fuel [31, 32]. The first part of this
104 study is dedicated to the oxidation of *n*-decane and to the impact on its stability of the addition of
105 different types of alcohols, at different proportions (1 – 20 %). Since the main autoxidation product
106 of hydrocarbons are hydroperoxides (ROOH), we systematically measured the total hydroperoxides
107 content of the fuel blends at the end of the PetroOxy tests using iodometry and potentiometric
108 titration. Several alcohol molecules have been studied at a temperature of 413 K and oxygen
109 pressure of 700 kPa. Several parameters in the alcohol chemical structures such as the size of the
110 chain (C_4 , C_6 , C_8 , C_{10}) in linear alcohols, the position of the OH group (*n*-butanol, butan-2-ol), and level
111 of branching in the hydrocarbon chain (*n*-butanol, iso-butanol, tert-butanol) were studied. *Ab initio*
112 calculations were performed to better understand the fundamental mechanisms underlying the
113 autoxidation experiments.

114

115 **EXPERIMENTAL METHODS**

116 PetroOxy device

117 Oxidation stability of fuel blends was tested in a PetroOxy from Anton Paar, one of the references of
118 the Rapid Small-Scale Oxidation Test of the ASTM D7545 methods [6, 7]. A 5 ml sample of liquid fuel
119 is placed in the gold-plated cell, which is then pressurized with pure O₂ under 7 bars and heated to
120 the test temperature (413 K here). The evolution of the pressure is recorded as a function of time
121 and the induction period is defined as the time required to achieve a 10% reduction in pressure in
122 the cell.

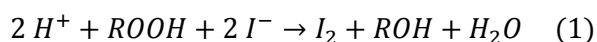
123 The viton o-ring sealing the cell was changed between each test and a careful cleaning of the reactor
124 was performed at the end of each experiment. Indeed, the use of alcohols in PetroOxy can lead to
125 small quantities of liquid condensates in the apparatus, which were found to affect the following IP
126 measurements.

127 Reactants

128 1-butanol (99.8 %), 1-decanol (≥ 99 %), tert-butanol (≥ 99.5 %), 2-butanol (99.5 %) and isobutanol
129 (99.5 %) were all anhydrous and purchased from Sigma Aldrich. 1-hexanol (99 %) came from Alfa
130 Aesar, *n*-decane (≥ 99 %) from Acros Chemicals, and 1-octanol (99 %) was provided by Fisher
131 Scientific. Potassium iodide (KI) anhydrous, and absolute ethanol were purchased from Carlo Erba.
132 Butylated hydroxytoluene (BHT) (≥ 99 %), triphenylphosphine (TPP) (reagent ≥ 99 %) and acetic acid
133 (≥ 99.8 %) were purchased from Sigma Aldrich.

134 Quantification of hydroperoxides

135 To determine the quantity of ROOH in fuels blends, the iodometric titration method from Roohi and
136 Rajabi [33] was used, but with a detection of the endpoint using potentiometry as proposed by Le et
137 al. [34]. This method allows to quantify the total amount of ROOH, by using the iodometric reaction:



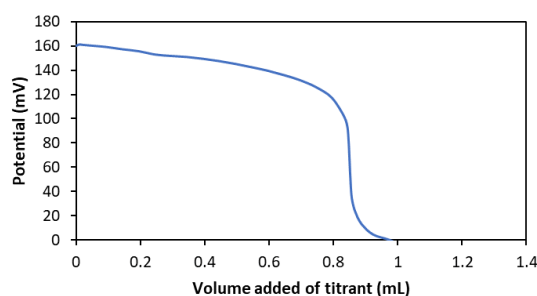
138 Around 0.5 g of KI is added to 30 mL of absolute ethanol in a beaker and 0.5 mL of acetic acid.
139 Potassium iodine acts as the source of iodine ions (I⁻) while acetic acid acts as a buffer and provides
140 H⁺ ions.

141 The reaction is complete after 15 min under agitation at 68°C, which means that one mole of ROOH
142 yields one mole of I₂. I₂ is thereafter determined using triphenylphosphine (TPP) as a titrant. The TPP
143 solution contains 0.08 M of TPP and 0.01 g of BHT to prevent oxidation of TPP [33]. A change of color
144 can be observed, as the solution turns from yellow to colorless, which indicates the endpoint of the
145 titration.



146 The endpoint was detected in this work using an automated potentiometric titrator (Mettler Toledo
147 G10S Compact Potentiometric Titrator), equipped with a Pt indicator electrode vs. an AgCl / Ag
148 reference electrode. Figure 1: shows an example of record given by the potentiometer.

149



150

151 *Figure 1: Titration result of oxidized pure n-decane after the PetroOxy test (413 K and 7 bar, IP = 182*
152 *min) titrated with TPP at 0,08 mol/L*

153 In a previous study, the uncertainty in [ROOH] was determined to mainly depend on the titration
154 endpoint volume and established that the global uncertainty in the potentiometer volume is ±0.04
155 mL [32].

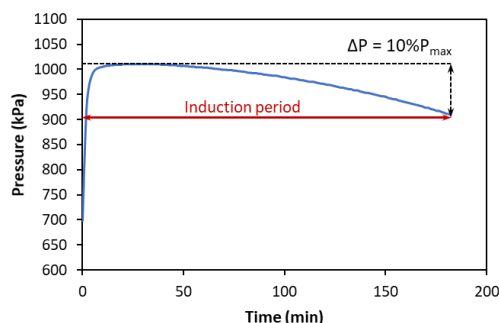
156 Uncertainties in the IP measures

157 During this study, we observed that the uncertainty varied with the different liquids tested in the
158 PetroOxy. For pure *n*-decane, the precision of the measurements was $\pm 2.5\%$, while for pure alcohols,
159 repeatability deteriorates and the uncertainty was between $\pm 5\%$ and $\pm 10\%$ for butanol isomers. 2-
160 butanol induced a higher uncertainty than other isomers and a specific discussion is held later in the
161 text. For blends, the uncertainty increased with the volume percentage of alcohols added in *n*-
162 decane. To be as precise as possible, every data including induction period of alcohol were given with
163 an extrapolation of the uncertainties of 10%. All the experimental measurements and their
164 repetitions are given in the supplemental material.

165 RESULTS AND DISCUSSION

166 1. Pure *n*-decane autoxidation

167 Figure 2 presents the pressure profile measured for a pure *n*-decane sample tested at 413 K.



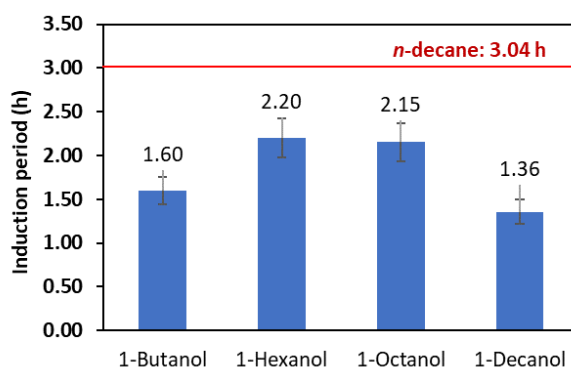
168

169 *Figure 2 : Induction period measurement with the PetroOxy device for *n*-decane at 413 K and 700 kPa*

170 The IP of pure *n*-decane is 182 minutes under the conditions of Figure 2. This value is in good
171 agreement with other *n*-decane IPs of the literature [7, 31].

172 2. Pure alcohol autoxidation: influence of the carbon chain length on the oxidation
173 stability

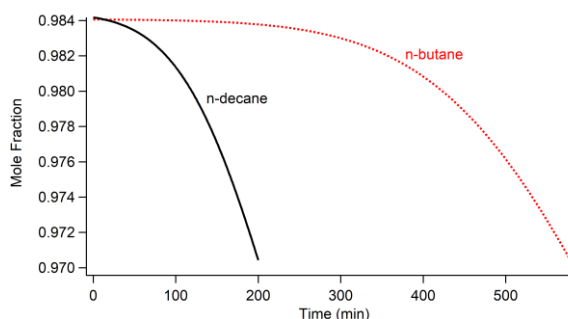
174 Pure 1-alcohols were first studied in the PetroOxy to compare their oxidation stability with pure *n*-
175 decane and to explore the effect of the chain length. Figure 3 presents the IP measured at 413 K and
176 7 bar of pure oxygen.



177
178 Figure 3: Induction period of pure 1-alcohols (413 K | 7 bar of O₂). The horizontal red line represents
179 the IP of pure *n*-decane.

180 It appears in Figure 3 that all the alcohols tested have an IP significantly lower than pure *n*-decane. 1-
181 butanol and 1-decanol feature the lower oxidation stabilities with a difference of more than 1 hour
182 compared to *n*-decane. The IPs of pure alcohols are shown to vary non-linearly with the length of the
183 carbon chain. Chatelain et al. [7] studied the impact of the chain length on the oxidation stability of
184 *n*-alkanes and found that the IP decreases nonlinearly with the number of carbon atoms from *n*-
185 hexane to *n*-hexadecane. A similar trend is observed here, from 1-hexanol to 1-decanol, even if the
186 values for 1-hexanol and 1-octanol are close. The fact that the IP of 1-butanol is lower than that of 1-
187 hexanol or 1-octanol cannot be compared with a similar case, involving *n*-hexane / *n*-octane and *n*-
188 butane because the latter is gaseous at standard conditions. Such a comparison can be made for
189 alkanes using simulations. Validated detailed kinetic models of *n*-butane and *n*-decane autoxidation
190 are available in the literature [32, 34] and they were used to simulate their autoxidation under
191 identical conditions (T = 413 K, [alkane] = 4.45 mol/L, [O₂] = 7.21×10⁻² mol/L). A homogeneous liquid

192 batch reactor (constant T, P, and V) solver based on Chemkin II library [35] was used with a constant
193 O₂ concentration [7, 14, 34]. Figure 4 presents the simulated conversion of *n*-decane and *n*-butane as
194 a function of time.



195

196 *Figure 4: Simulated n-butane and n-decane conversion during their liquid phase oxidation at 413 K.*

197 Figure 4 demonstrates that the rate of conversion of *n*-decane is much higher than that of *n*-butane.

198 A qualitative link with the IP can be made: the conversion and the rate of oxidation of the fuel as

199 measured in the PetroOxy cell by the oxygen pressure drop are directly linked and the higher the

200 conversion rate, the lower the IP [7]. If we observe fuel consumption rates at 40 minutes, where the

201 fuel conversions are almost zero, it can be seen that both fuels are entirely consumed by the H-

202 abstractions reactions $\text{RH} + \text{ROO}\bullet \rightarrow \text{R}\bullet + \text{ROOH}$. For *n*-butane, the total rate of consumption is $2.3 \times$

203 $10^{-13} \text{ mol cm}^3 \text{ s}^{-1}$ while for *n*-decane, it is $3.2 \times 10^{-12} \text{ mol cm}^3 \text{ s}^{-1}$. The total rate of consumption of *n*-

204 butane is 91% by secondary H-atom abstractions and 9% by primary H-atom abstractions by a $\text{ROO}\bullet$

205 radical, which is mostly the secondary peroxy butyl radical. For *n*-decane, a similar behavior is

206 observed, the total rate of consumption is 94 % by secondary H-atom abstractions and 2.1% by the

207 primary H-abstractions by $\text{ROO}\bullet$. *n*-butane contains 4 secondary H-atoms, that are abstracted at a

208 total rate of $2.1 \times 10^{-13} \text{ mol cm}^3 \text{ s}^{-1}$, which correspond to a rate of 5×10^{-14} per secondary H-atom. *n*-

209 decane possesses 16 secondary H-atoms, all abstracted at a total rate $3.0 \times 10^{-12} \text{ mol cm}^3 \text{ s}^{-1}$, which

210 correspond to a rate of about $2 \times 10^{-13} \text{ mol cm}^3 \text{ s}^{-1}$ per secondary H-atom. At 413 K, the ratio of the

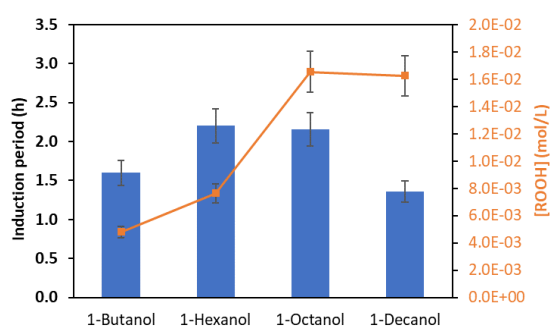
211 rate constants of H-abstraction by $\text{ROO}\bullet$ from the fuel in *n*-decane over the one in *n*-butane is 2.3,

212 which is close to the ratio of 3.6 for the rates of abstraction per H-atom (*n*-decane / *n*-butane). This

213 demonstrates that, under these conditions, the higher rate of consumption of *n*-decane is mostly
214 explained by its higher number of H-atoms compared to *n*-butane.

215 This analysis raises an interesting question on the higher reactivity (shorter IP) of *n*-butanol
216 compared to *n*-octanol. It can be hypothesized that the main consumption path of *n*-butanol is not
217 the same as the one established in *n*-alkanes. As the size of the alcohol increases, two consumption
218 fluxes may exist: the one specific to alcohol and the one observed for alkanes. This may explain the
219 trends observed in Figure 3. This point will be further discussed in the last section of the manuscript.

220 Since the total ROOH concentration were quantified at the end of each IP measure, the impact of the
221 alcohol size on the [ROOH] values can also be determined, as shown in Figure 5.



222
223 *Figure 5: Evolution of total hydroperoxide concentration (right axis) measured at the IP time as a*
224 *function of the linear alcohol size. Left axis is the corresponding induction period measured at 413 K*
225 *and 7 bar of O₂.*

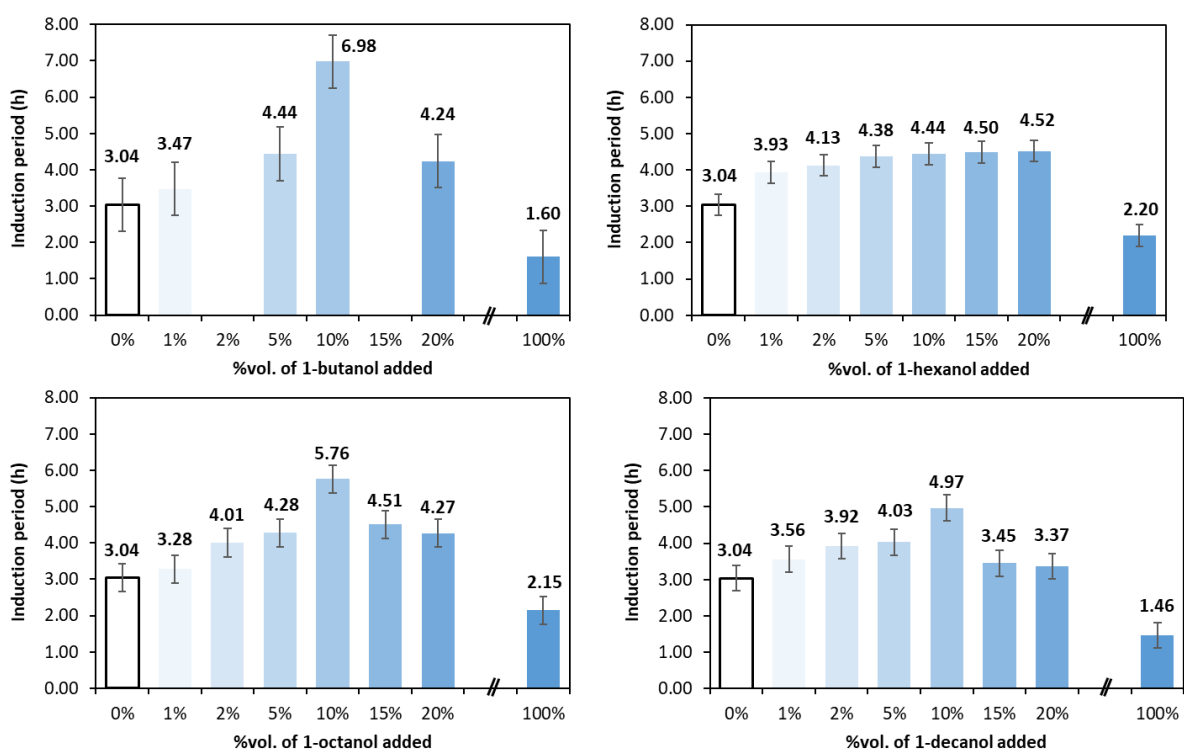
226 The experimental data presented in Figure 5 show that total concentration of ROOH measured at the
227 IP time increases with the length of the linear alcohol, by a factor of 2.7, from *n*-butanol to *n*-octanol,
228 then remains approximately constant for decanol. This further supports the hypothesis that a specific
229 mechanism occurs for alcohols, which is more marked for short chains, that leads to a decrease in
230 the amount of total hydroperoxides compared to longer chain alcohols or alkanes (total [ROOH] in *n*-
231 decane at the IP time is about 8×10^{-2} mol/L [34]).

232 Figure 5 shows that all the alcohols tested have a shorter IP than pure *n*-decane. In the following
 233 section, we explore the effect of the addition of a linear alcohol on the IP of *n*-decane, for different
 234 proportions of 1-butanol, 1-hexanol, 1-octanol and 1-decanol.

235

236 *3. Influence of the quantity of alcohols on the induction period of n-decane*

237 The evolution of the measured IPs at 413 K under 7 bar of O₂ for linear alcohols (1-butanol, 1-
 238 hexanol, 1-octanol, 1-decanol) blended with *n*-decane (x % alcohol in (100-x) %vol. *n*-decane) are
 239 presented in Figure 6.



240

241 *Figure 6: Induction period of alcohol / n-decane blends for different volume percentages of alcohol*

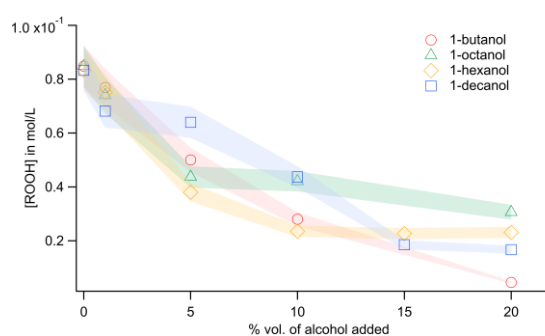
242

(413 K | 7 bar)

243 We have already mentioned that the IPs of pure alcohols are always lower than that of pure *n*-
 244 decane and this can be seen at the limits of the x-axis. It can also be noted that for all proportions of
 245 any alcohol added, up to 20 %vol., the IP of the blend increases compare to pure *n*-decane, which

246 demonstrate that these alcohols are increasing its thermal oxidation stability. This antioxidant-like
 247 effect is observed only for alcohols among the diverse families of biofuels (FAME, ether and ketone)
 248 [19, 24]. The addition of 1% of alcohol is sufficient to increase the IP of *n*-decane by 10 to 30%
 249 depending on the alcohol. Figure 6 also shows that the increase in the IPs of *n*-decane/alcohol
 250 blends varies in a non-monotonic way with the proportion of alcohol added. Over the full range of
 251 proportion of alcohols added, from 1 to 20%, the IP increases, reaches a maximum value and
 252 decreases. *n*-hexanol seems to behave differently from the others, and we think that it may either
 253 reach a maximum IP value for a proportion of 20% or higher, or that the uncertainties in the IPs
 254 mean that this maximum cannot be clearly established. We observe a maximum increase in the IP for
 255 the addition of 10% of 1-butanol, 1-octanol and 1-decanol in *n*-decane.

256 **Erreur ! Source du renvoi introuvable.** presents the total ROOH concentration of aged fuels
 257 measured at the IP time for different proportions of alcohols blended to *n*-decane.



258
 259 *Figure 7 : Total ROOH concentration (potentiometric titration with TPP) at the IP time as a function of*
 260 *the %vol. of alcohol added. Open symbols are the experimental values and shaded areas at the same*
 261 *x-axis coordinate represent uncertainties. Shaded areas between the symbols are drawn to guide the*
 262 *eyes.*

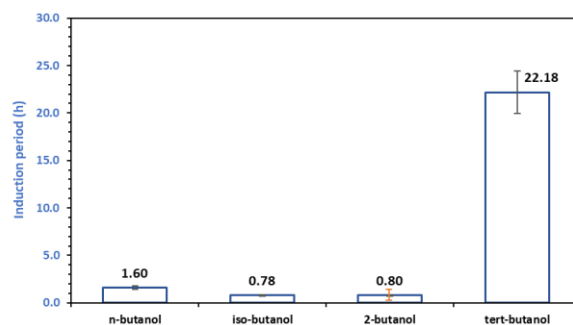
263 The ROOH concentration at the IP time (noted $[ROOH]_{IP}$) decreases with the addition of any linear
 264 alcohol compared to the case of pure *n*-decane. The addition of 1% of alcohol decreases the total
 265 ROOH concentration by about 12% (mean value for the four alcohols) compared to *n*-decane while
 266 for 20% added, the total $[ROOH]_{IP}$ is divided by a mean factor of 7.5 if all alcohols are considered.
 267 Figure 7 shows that, for 20% of alcohol added, 1-butanol has the most pronounced $[ROOH]_{IP}$ -

268 lowering effect (a factor of 19 compared to pure *n*-decane) while larger alcohols have [ROOH]_{IP}-
269 lowering factors of about 3 to 5.

270 The experimental measures of [ROOH]_{IP} for the different blends reinforce the hypothesis of an
271 alternative mechanism for the liquid-phase oxidation of alcohols compared to alkanes. Figure 7
272 shows that the addition of alcohol to *n*-decane induces a decrease in the total concentration of
273 hydroperoxides (ROOH and HOOH). The greater the proportion added, the greater the decrease, up
274 to 20%. This strongly suggests that the classical chemical scheme that explains ROOH formation
275 during the autoxidation of alkanes ($R\bullet + O_2 \rightarrow ROO\bullet$ and $RH + ROO\bullet \rightarrow R\bullet + ROOH$) is in competition
276 with another reaction route when linear alcohols are present in the mixture, which is specific to them
277 and does not solely yield hydroperoxides. We will propose a detailed discussion of this new pathway
278 in the last section of this paper, but given the marked antioxidant effect of butanol, it seems clear
279 that there is an easy abstraction of H-atoms in β -position relative to the OH group. The reaction
280 $HORH + ROO\bullet \rightarrow HOR\bullet + ROOH$ competes with $RH + ROO\bullet \rightarrow R\bullet + ROOH$. If in the latter reaction, the
281 alkyl radical $R\bullet$ regenerates an $ROO\bullet$ radical by addition on O_2 , in the case of linear alcohols, the
282 $HOR\bullet$ either does not solely leads to the formation of a $HOROO\bullet$ radical through its reaction with O_2
283 or the fate of $HOROO\bullet$ is not to be solely consumed by H-abstraction with the fuel. We propose that
284 the elimination of hydroperoxyl radical $HOROO\bullet \rightarrow R(C=O) + HOO\bullet$ is in competition with the H-
285 abstraction flux that forms hydroperoxides $RH + HOROO\bullet \rightarrow R\bullet + HOROOH$. To further explore this
286 hypothesis, we performed thermal oxidation stability experiments on the different butanol isomers.

287 4. Thermal oxidation stability of butanol isomers

288 The influence of the branching and the position of the OH group in alcohols was probed using the
289 isomers of butanol. We first present the results for the pure components. The induction periods of
290 pure butanol isomers are represented in Figure 8.



291

292

Figure 8: Induction periods of the isomers of butanol, 413 K and 7 bar of O_2

293 The induction periods of *iso*- and 2-butanol appear to be similar and slightly shorter than 1-butanol

294 while the IP of *tert*-butanol is significantly longer. It should be noted that experiments with 2-butanol

295 led to repeatability problems or failed tests in the PetroOxy. For example, some tests with pure 2-

296 butanol led to a very short IP of 15 minutes. Since 2-butanol came from the same bottle for every

297 test, the issues may come from either impurity in the PetroOxy cell and/or the oxygen alimentation

298 line or an increased leaking of the cell with this type of alcohol. These results should therefore be

299 treated with caution. In the case of *tert*-butanol, which is solid below 299 K, PetroOxy experiments

300 were performed when the room temperature was above this temperature. Among the different

301 issues that can occur for PetroOxy experiments with pure alcohol is their highest vapor pressure

302 compared to *n*-decane or petroleum products for which this test was designed. Table 1 presents the

303 vapor pressures of the different isomers of butanol and *n*-decane at room and PetroOxy

304 temperatures.

305 Table 1: Vapor pressures (atm) of butanol isomers and *n*-decane from Simulis [36].

Compound	P_{sat} (300 K) in atm	P^{sat} (413 K) in atm
<i>n</i> -decane	2.0×10^{-3}	0.38
1-butanol	1.0×10^{-2}	2.07
<i>iso</i> -butanol	1.6×10^{-2}	2.86
2-butanol	2.6×10^{-2}	3.58
<i>tert</i> -butanol	6.2×10^{-2}	6.20

306

307 Table 1 shows that at room temperature, all the isomers of butanol have a vapor pressure higher
308 than *n*-decane by at least a factor of 5. For 2-butanol and *tert*-butanol, P_{sat} at 300K are, respectively
309 13 and 31 times higher than that of *n*-decane. During the first stage of the PetroOxy test, the cell is
310 sealed and filled with oxygen. It is therefore possible that butanol may enter the oxygen supply line
311 and perturb the subsequent experiments. Despite a specific procedure including thorough cleaning
312 and several runs with our calibration fluid between butanol tests, the repeatability issues with 2-
313 butanol could not be resolved. When the PetroOxy cell reaches the desired pressure, the
314 temperature is increased to 413 K in a few minutes. Vapor pressures at this temperature (Table 1)
315 show that 2- and *tert*-butanol will strongly contribute to the pressure signal, this is also the case for
316 1- and *iso*-butanol, but in a lesser extent. This may also contribute to the perturbation of the
317 PetroOxy test through an alteration of the O-rings, that would increase the leaking rate of the cell. To
318 verify this hypothesis, a leak test was carried out in which the stability of each fuel was
319 tested under 7 atmospheres of inert gas (N_2). Under these conditions, the rate of leakage of
320 2-butanol (0.048 bar/hour) is 2.75 higher than that of *n*-decane (0.018 bar/hour). Table S1
321 gives all the experimental data and the associated uncertainties.

322 Despite the uncertainties observed for 2-butanol, a clear difference is established between *tert*-
323 butanol and the other alcohols. Since *tert*-butanol is the only isomer that does not have a hydrogen
324 atom on the carbon bearing the OH group, its autoxidation mechanism is different than the other
325 isomers and it leads to a higher oxidation stability. As already mentioned, at these temperatures, the
326 H-abstraction of the H-atoms in β -position of the OH group are probably dominant with kinetic rate
327 constants that are higher than those for *n*-decane (secondary H-atoms). This is consistent with the
328 antioxidant effect observed for linear alcohols that requires an easiest H-atom to be abstracted
329 compared to the H-atoms of *n*-decane.

330 Iodometry and potentiometric titration with TPP of butanol isomers at the end of the PetroOxy test
331 (at the IP time) showed that the total $[\text{ROOH}]_{\text{IP}}$ is similar for 1- and *iso*-butanol but that no
332 hydroperoxides could be detected for 2- and *tert*-butanol. If it is not surprising in the case of *tert*-
333 butanol which has a very long IP and therefore a long buildup of ROOH, it is more surprising for 2-
334 butanol. Again, the latter isomer has a singular behavior in our experiments. Since the IP of 2-butanol
335 is short compared to *n*-decane, it can be assumed that the oxidation mechanism of 2-butanol either
336 does not involve the formation of hydroperoxides, which is highly unlikely, or leads to fragile
337 hydroperoxides that decompose rapidly.

338 5. Mechanism of alcohols oxidation, pure and in *n*-decane

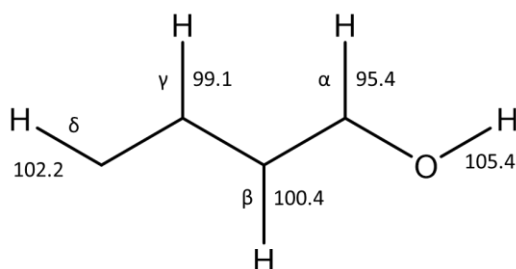
339
340 Our experimental results show that pure alcohols have a lower oxidation stability (IP) than pure *n*-
341 decane. However, when 1 to 20% vol. alcohol is added to *n*-decane, a stability-enhancing effect (IP
342 increases) is observed. This increase of IP is accompanied by a decrease of the total content of
343 hydroperoxides at the IP time. This suggests that an anti-oxidant like behavior is occurring when
344 alcohols are added to *n*-decane. The functioning of an antioxidant is based on the existence of a
345 labile hydrogen atom in its molecular structure, where the H-abstractions of the chain carrier radicals
346 ($\text{ROO}\cdot$ in most cases) will be faster than those from the fuel. H-abstractions from the antioxidant
347 leads to a radical that does not contribute to the propagation loop that consumes the fuel and slows
348 down the global autooxidation reaction. To verify this hypothesis, we calculated the bond
349 dissociation energy of C-H bonds in 1-butanol, in the gas phase and in *n*-decane and 1-butanol
350 solvents.

351 Gas phase enthalpies of 1-butanol, its radicals, and the H-atom were computed at the QCISD(T)/cc-
352 PV ∞ QZ//B2PLYPD3/6-311+G(2d,p) level of theory using Gaussian16 software [37]. More details on
353 this level of calculation can be found elsewhere [38, 39] and here we only recall its main features.
354 Geometry optimization and frequency calculations are performed at the B2PLYPD3/6-311+G(2d,p)
355 level of theory. Single point energy calculations are done on the optimized geometries at the

356 QCISD(T)/cc-pVTZ, QCISD(T)/cc-pVDZ and MP2/cc-pVQZ levels of theory that are used to compute
 357 QCISD(T)/cc-PV ∞ QZ energies. Enthalpies given by Gaussian were used for the calculation of the gas
 358 phase Bond Dissociation Energy (BDE). Solvation enthalpies ($\Delta_{\text{solv}}H^\circ$) of 1-butanol and its radicals
 359 were computed with COSMOthermX version C30_1602 [40]. Cosmo input files of radicals were
 360 generated with TMoleX version 4.0.1 [41] using the BP/TZVP method. Gibbs free energies of
 361 solvation were computed with COSMOthermX as a function of temperature (293 to 303 K), which
 362 was then used to calculate the entropy of solvation ($\Delta_{\text{solv}}S$) and $\Delta_{\text{solv}}H^\circ$. The BDE, for the reaction RH
 363 $\rightarrow \text{R}\cdot + \text{H}\cdot$, in the liquid phase is defined as $\text{BDE}_{\text{gas}} + \Delta_r\Delta_{\text{solv}}H^\circ$, where $\Delta_r\Delta_{\text{solv}}H^\circ$ is equal to:

$$\Delta_r\Delta_{\text{solv}}H^\circ = \Delta_{\text{solv}}H^\circ(\text{R}\cdot) + \Delta_{\text{solv}}H^\circ(\text{H}\cdot) - \Delta_{\text{solv}}H^\circ(\text{RH}) \quad (3)$$

367 Figure 9 presents the computed BDE in the gas phase.



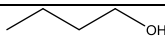
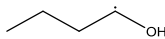
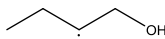
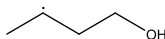
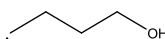
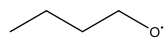
368
 369 *Figure 9: Gas phase C-H BDEs in kcal mol⁻¹ computed at the QCISD(T)/cc-PV ∞ QZ//B2PLYPD3/6-311+G(2d,p) level of theory*

371 Our computed C-H BDEs agree with the *ab initio* calculated data of the literature. For example, a
 372 mean deviation of only 0.3 kcal/mol is observed with the BDE computed by Oyeyemi et al. [42] with
 373 the high-level, multireference averaged coupled-pair functional (MRACPF2) method. It is well known
 374 that C-H bonds in α -position of the OH groups have a lower BDE than a corresponding bond in *n*-
 375 alkanes. Here, we can see that in the gas-phase, the BDE of the α -C-H bond is 3.7 kcal mol⁻¹ lower
 376 than the γ -C-H bond that is equivalent to a secondary C-H bond in a linear alkane (99.1 kcal mol⁻¹ *n*-
 377 heptane and *n*-octane [43]). H-abstractions by radicals will therefore be favored at the α position.

378 Conversely, the BDE of the β -C-H bond is higher compared to *n*-alkanes. Thus, the corresponding H-
 379 abstraction involves a higher energy barrier, which reinforces the role of the alcohol function,
 380 particularly for short-chain alcohols.

381 To the best of our knowledge, no BDE data are available for 1-butanol in the condensed phase. Table
 382 2 presents the thermochemical solvation data computed with COSMOTermX for 1-butanol and its
 383 radicals.

384 *Table 2 : Solvation quantities computed with COSMOTermX at the BP/TZVP level of theory at 298.15 K (see*
 385 *text).*

Molecular structure	<i>n</i> -decane solvent			1-butanol solvent		
	$\Delta_{\text{solv}}G^\circ$ (kcal/mol)	$\Delta_{\text{solv}}S^\circ$ (cal/mol.K)	$\Delta_{\text{solv}}H^\circ$ (kcal/mol)	$\Delta_{\text{solv}}G^\circ$ (kcal/mol)	$\Delta_{\text{solv}}S^\circ$ (cal/mol.K)	$\Delta_{\text{solv}}H^\circ$ (kcal/mol)
	-3.3	-9.8	-6.3	-6.1	-23.1	-12.9
	-3.1	-9.6	-5.9	-6.4	-26.2	-14.2
	-3.5	-9.7	-6.4	-6.5	-24.1	-13.7
	-3.2	-9.7	-6.1	-6.1	-23.9	-13.2
	-3.3	-9.7	-6.2	-6.2	-23.7	-13.3
	-3.2	-9.5	-6.1	-3.9	-8.8	-6.5
H \cdot	1.5	-6.8	-0.5	1.4	-6.1	-0.4

386
 387 In the CompSol experimental database [44], Gibbs free energies of solvation are available for 1-
 388 butanol as a solute in *n*-decane and 1-butanol solvents, respectively. $\Delta_{\text{solv}}G$ of 1-butanol in *n*-decane
 389 is $-3.6 \text{ kcal mol}^{-1}$ at 293.15 K, which is close to our value presented in Table 2 ($-3.3 \text{ kcal mol}^{-1}$ at
 390 298.15 K). The experimental $\Delta_{\text{solv}}G$, $\Delta_{\text{solv}}H$ and $\Delta_{\text{solv}}S$ of 1-butanol solute in 1-butanol solvent (pure
 391 compound data) are $-6.1 \text{ kcal mol}^{-1}$, $-12.3 \text{ kcal mol}^{-1}$ and $-20 \text{ cal mol}^{-1}\text{K}^{-1}$ at 298.15 K, which are in
 392 remarkable agreement with our computed data (top row, right side). Using $\Delta_{\text{solv}}H^\circ$ and the calculated
 393 gas-phase BDEs, we computed the BDE of 1-butanol in these two solvents (Table 3).

394

395

396 *Table 3: Computed bond dissociation energies of 1-butanol in the gas- and liquid-phases (QCISD(T)/cc-*397 *PV ∞ QZ//B2PLYPD3/6-311+G(2d,p) for gas phase and COSMOTermX BP-TZVP for $\Delta_{solv}H^\circ$, see text)*

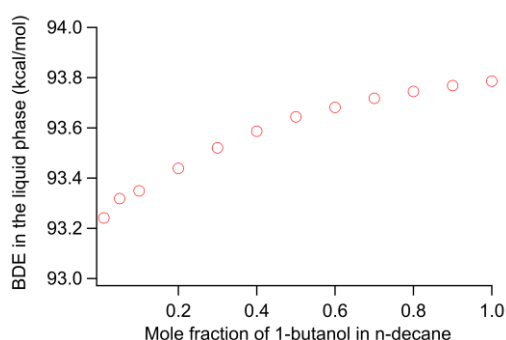
Bond Dissociation Energies (kcal mol ⁻¹)			
C-H bond	Gas phase	<i>n</i> -decane solvent	1-butanol solvent
α	95.4	95.3	93.8
β	100.4	99.8	99.2
γ	99.1	98.7	98.4
δ	102.2	101.8	101.4
O-H	105.4	105.1	111.4

398

399 The computed BDEs presented in Table 3 clearly show that the change from gas to liquid phase, in
400 the *n*-decane solvent, has a very small effect. All the BDEs in *n*-decane are lower than the gas phase
401 one by a mean value of 0.4 kcal mol⁻¹, which falls within the uncertainty of our calculations. Going
402 from gas to liquid 1-butanol solvent has a stronger effect on the C-H BDEs and the effect is very
403 strong for the BDE of the O-H bond which is increased by 6 kcal mol⁻¹ because of hydrogen bonding in
404 the condensed phase. We also observe that the closer the C-H bond is to the hydroxyl group, the
405 greater the effect of gas to liquid change. The BDE of the α -C-H bond in pure, liquid, 1-butanol is 1.6
406 kcal mol⁻¹ below the value in the gas phase. From an energy point of view, this means that the α -H-
407 atom abstraction in liquid 1-butanol is even easier than in the gas phase. The differences in the BDE
408 of a C-H_{secondary} bond in *n*-decane and the α -C-H bond in 1-butanol (and all the other alcohols studied)
409 is probably the main cause of the highest reactivity of pure alcohols compared to *n*-decane (Figure 6)
410 because H-abstractions from the fuel will be easier.

411 Since several oxidation stability experiments were performed for *n*-decane / 1-butanol mixtures, we
412 also computed the variations in α -C-H BDE as a function of the proportion of 1-butanol added in
413 *n*-decane (Figure 10).

414



415

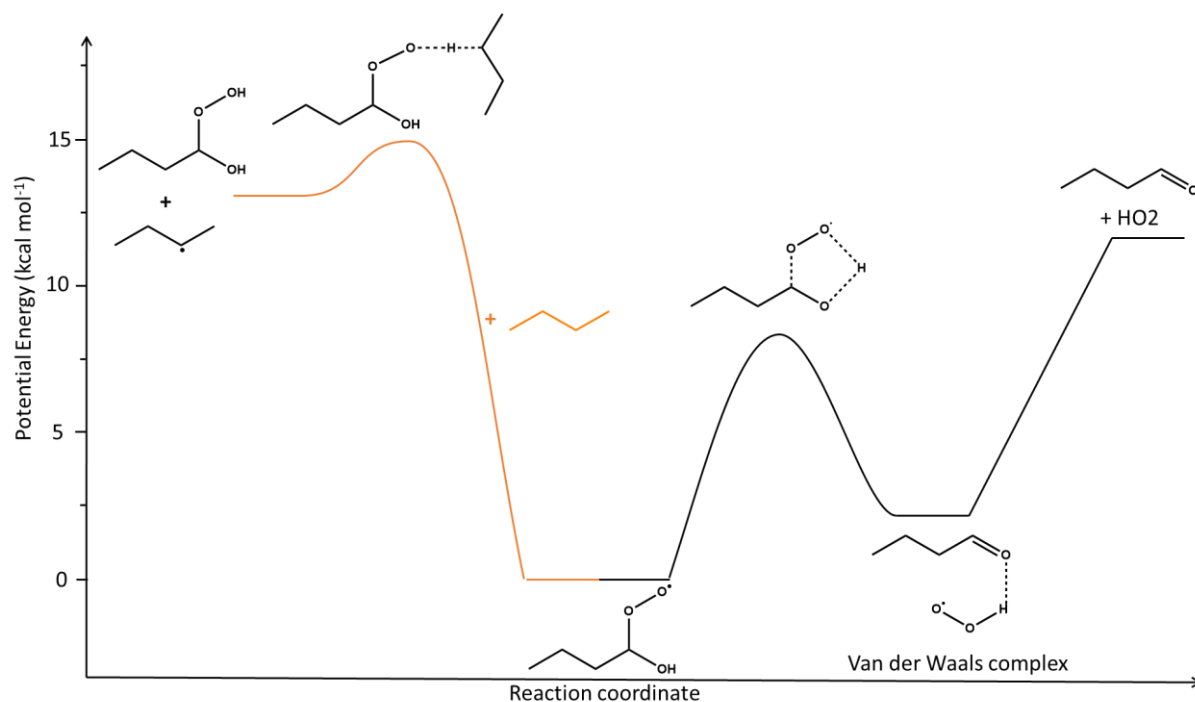
416 *Figure 10: Evolution of the α -C-H BDE in 1-butanol as a function of the composition of n-decane/1-*
417 *butanol mixtures*

418 In Figure 10, it can be seen that, starting from $X_{1\text{-butanol}} = 1$ (α -C-H BDE of pure butanol) to $X_{1\text{-butanol}} =$
419 0.01, a decrease of $0.5 \text{ kcal mol}^{-1}$ of the α -C-H BDE is observed. The BDE of the α -C-H bond is affected
420 by the composition of the mixture, and the smaller the proportion of 1-butanol in *n*-decane, the
421 lower the BDE value. The antioxidant effect of alcohol in *n*-decane is therefore further favored by the
422 thermochemistry for the smaller proportions.

423 1-hydroxybutyl α -radical will be the only radical from 1-butanol formed at the temperatures of our
424 experiments. Its oxidation will lead to the formation of a α -hydroxybutyl peroxy radical: $\text{HOR}\bullet + \text{O}_2$
425 $\rightarrow \text{HOROO}\bullet$. In the case of pure *n*-decane, the $\text{ROO}\bullet$ radicals are mainly consumed by H-abstractions
426 from the fuel ($\approx 80\%$ of their total consumption flux at 413 K) [34], yielding all hydroperoxides
427 measured at IP times. Our experimental results show that a competitive reaction is occurring for
428 pure alcohols. We therefore investigated the potential energy surfaces (PES) for the H-abstraction RH
429 $+ \text{HOROO}\bullet \rightarrow \text{R}\bullet + \text{HORO}OH$ and the competitive unimolecular decomposition $\text{HOROO}\bullet \rightarrow \text{R}(\text{C}=\text{O}) +$

430 HOO•, which leads to less reactive species as discussed below. Figure 11 presents the PES computed
431 at the B2PLYPD3/6-311+G(2d,p) level of theory.

432



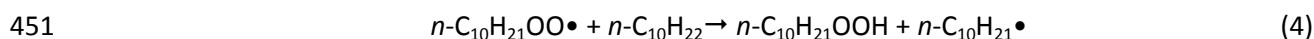
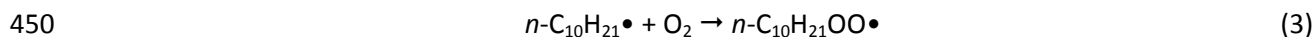
433

434 *Figure 11: Potential energy surface at 0 K of the HO₂ elimination in α-hydroxybutyl peroxy radical and*
435 *its H-abstraction from n-butane. PES computed at the B2PLYPD3/6-311+G(2d,p) level of theory in gas*
436 *phase.*

437 The PES presented in Figure 11 shows that the HO₂• elimination in α-hydroxybutyl peroxy faces a
438 very low energy barrier of 8.4 kcal mol⁻¹. This reaction leads to a Van der Waals post-reactive
439 complex that can decompose into butanal and HO₂•, which lie 11.7 kcal mol⁻¹ above the initial peroxy
440 radical. The other part of the PES (orange line) show that the H-abstraction from n-butane (used here
441 as a model for n-decane or any n-alkanes) has an energy barrier of 13.9 kcal mol⁻¹ and leads to
442 products lying 13.0 kcal mol⁻¹ above the entrance channel (α-hydroxybutyl peroxy + n-butane). From
443 a pure potential energy point of view, our calculations demonstrate that HO₂• elimination will be
444 greatly favored at autoxidation temperatures. In order to confirm this hypothesis at the kinetic level,

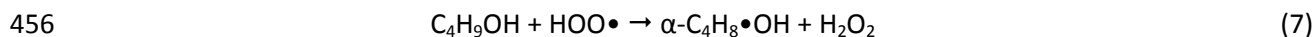
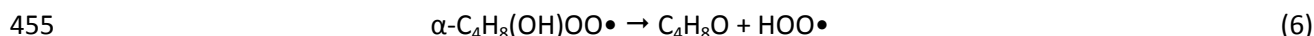
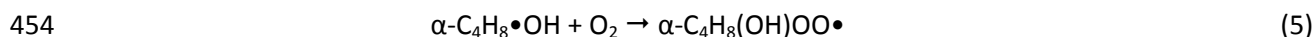
445 entropic effects on these reactions and concentration effects on the bimolecular reaction rate need
446 to be taken into account.

447 Experimental results and *ab initio* calculations allow us to propose an explanation for the behavior of
448 alcohols, pure and blended with *n*-decane. The main consumption flux of *n*-decane (long chain
449 mechanism) during its autoxidation are the propagations (3-4):

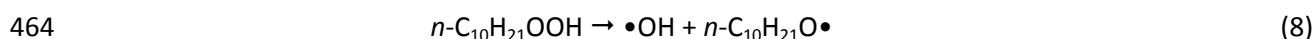


452 Reaction (4) regenerates an alkyl radical that yields a peroxy decyl radical in reaction (3).

453 In the case of butanol, this propagation loop is different and involves 3 reactions:



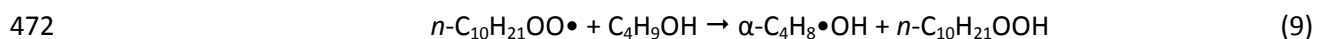
457 where $\alpha\text{-C}_4\text{H}_8\bullet\text{OH}$ is the α -hydroxybutyl radical and $\text{C}_4\text{H}_8\text{O}$ is the butanal. In this mechanism, the
458 peroxy radical does not leads to the formation of an hydroperoxide, but it decomposes into butanal
459 and $\text{HO}_2\bullet$. The latter radical can abstract an H-atom from the alcohol and yield hydrogen peroxide.
460 The latter molecule is known to be much more stable than hydroperoxides with BDEs of the O—O
461 bond of $50.35 \text{ kcal mol}^{-1}$ and 43 kcal mol^{-1} , respectively [43]. H_2O_2 is stable at autooxidation
462 temperatures whereas hydroperoxides such as $n\text{-C}_{10}\text{H}_{21}\text{OOH}$ decompose slowly and act as
463 degenerate branching agents, which increase the number of free radicals in the liquid:



465 Pure alcohols were shown to have a lower stability than *n*-decane and our BDE calculations show
466 that it can be explained by the difference between the BDE of a secondary C-H bond in *n*-decane and
467 the α -C-H bond in butanol. Since the fuel consumption mainly occurs by H-abstractions (by $\text{ROO}\bullet$ or

468 HOO• radicals in these cases) the lowest BDE of the α -C-H bond increases the rate of alcohol
469 consumption compared to *n*-decane.

470 This low BDE in alcohol is also responsible for the antioxidant effect observed when they are added in
471 moderate amounts to *n*-decane. The propagation loop (3-4) is interrupted by reaction (9):



473 Once formed, the $\alpha\text{-C}_4\text{H}_8\cdot\text{OH}$ radical reacts with O₂ to follow the mechanism of reactions (5-7). This
474 slows down the consumption of *n*-decane and produces more stable H₂O₂ peroxides.

475 CONCLUSION

476 The oxidation stability of pure alcohols and their mixtures in *n*-decane was investigated
477 experimentally in a PetroOxy. At the induction period time, the total content of hydroperoxides was
478 also determined by iodometry and potentiometry. Experiments show that pure, linear and lightly
479 branched alcohols have a lower oxidation stability than *n*-decane. For linear alcohols, as the length of
480 the carbon chain increases from 1-butanol to 1-decanol, the IP first increases from C₄ to C₆, and then
481 decreases from C₆ to C₁₀. This behavior is similar to that observed in *n*-alkanes and was explained by
482 our simulations by the higher number of H-atoms that can be abstracted as the size of the chain
483 increases. 1-butanol has been shown to be a special case as its IP is shorter than that of the other
484 linear alcohols. We explained this behavior by a specific mechanism of alcohol autoxidation, involving
485 an easier H-abstraction from the H-atoms linked to the carbon bearing the OH group. Our theoretical
486 calculations showed that the bond dissociation energy of these C-H bonds is lower than the
487 corresponding C—H bond in *n*-decane, in both gas and condensed phases (in *n*-decane and 1-butanol
488 liquids). Influence of the branching level of pure alcohols on their oxidation stability was explored
489 with the isomers of butanol. Experimental results showed that if no H-atom are available in α -
490 position of the OH group, the stability is considerably higher.

491 The addition of linear alcohol fuels to *n*-decane enhances its oxidation stability and this antioxidant
492 effect is found to depend non-linearly with the proportion added. In general, a maximum
493 enhancement of the stability is found for 10 % volume addition. Based on theoretical calculations, we
494 explain that this behavior is due to the easy abstraction of H-atoms in the α -position of the OH group
495 that interrupts the propagation loop that mostly contributes to the conversion of *n*-decane. The
496 formation of the α -centered alcohol radical leads to the formation of a peroxy radical, which mostly
497 decomposes into an aldehyde and HO₂• instead of contributing to the fuel consumption by H-
498 abstractions. Theoretical calculations showed that this pathway is favored from a potential energy
499 point of view and contributes to slow down the conversion of liquid *n*-decane at low temperatures.

500 **ACKNOWLEDGMENTS**

501 The project leading to this application has received funding from the European Research Council
502 (ERC) under the European Union's Horizon 2020 research and innovation program (grant agreement
503 No 101003318). This work was also financially supported by the BioACe project, grant ANR-18-CE05-
504 002 of the French National Research Agency, and by the Grand-Est region. This project was provided
505 with computer and storage resources by GENCI at IDRIS thanks to the grant 2023-AD010812434R2 on
506 the supercomputer Jean Zay.

507 **REFERENCES**

- 508 [1] Cabrera E, de Sousa JMM. Use of Sustainable Fuels in Aviation - A Review. *Energies*
509 2022;15(7):2440.
- 510 [2] Bergthorson JM, Thomson MJ. A review of the combustion and emissions properties of
511 advanced transportation biofuels and their impact on existing and future engines. *Renewable*
512 *and Sustainable Energy Reviews* 2015;42:1393-417.
- 513 [3] Westbrook CK. Biofuels Combustion. *Annual Review of Physical Chemistry* 2013;64(1):201-
514 19.
- 515 [4] Hazlett R. *Thermal Oxidation Stability of Aviation Turbine Fuels*. 1991.
- 516 [5] Jia T, Zhang X, Liu Y, Gong S, Deng C, Pan L, et al. A comprehensive review of the thermal
517 oxidation stability of jet fuels. *Chemical Engineering Science* 2021;229:116157.
- 518 [6] Aminane S, Sicard M, Melliti Y, Ser F, Sicard L. Experimental study of the kinetics of
519 degradation of *n*-dodecane under thermo-oxidative stress at low temperature and
520 mechanism inferred. *Fuel* 2022;307:121669.

- 521 [7] Chatelain K, Nicolle A, Ben Amara A, Catoire L, Starck L. Wide Range Experimental and Kinetic
522 Modeling Study of Chain Length Impact on n-Alkanes Autoxidation. *Energy & Fuels*
523 2016;30(2):1294-303.
- 524 [8] DeWitt MJ, West Z, Zabarnick S, Shafer L, Striebich R, Higgins A, et al. Effect of Aromatics on
525 the Thermal-Oxidative Stability of Synthetic Paraffinic Kerosene. *Energy & Fuels*
526 2014;28(6):3696-703.
- 527 [9] Corporan E, Edwards T, Shafer L, DeWitt MJ, Klingshirn C, Zabarnick S, et al. Chemical,
528 Thermal Stability, Seal Swell, and Emissions Studies of Alternative Jet Fuels. *Energy & Fuels*
529 2011;25(3):955-66.
- 530 [10] Heneghan SP, Zabarnick S. Oxidation of jet fuels and the formation of deposit. *Fuel*
531 1994;73(1):35-43.
- 532 [11] Russell GA. Deuterium-isotope Effects in the Autoxidation of Aralkyl Hydrocarbons.
533 Mechanism of the Interaction of Peroxy Radicals¹. *Journal of the American Chemical Society*
534 1957;79(14):3871-7.
- 535 [12] Denisov ET, Afanas' ev IB. Oxidation and antioxidants in organic chemistry and biology. CRC
536 press, Boca Raton; 2005.
- 537 [13] Chatelain K, Nicolle A, Ben Amara A, Starck L, Catoire L. Structure–Reactivity Relationships in
538 Fuel Stability: Experimental and Kinetic Modeling Study of Isoparaffin Autoxidation. *Energy &*
539 *Fuels* 2018;32(9):9415-26.
- 540 [14] Jalan A, West RH, Green WH. An Extensible Framework for Capturing Solvent Effects in
541 Computer Generated Kinetic Models. *The Journal of Physical Chemistry B* 2013;117(10):2955-
542 70.
- 543 [15] Zabarnick S, West ZJ, Arts A, Griesenbrock M, Wrzesinski P. Studies of the Impact of Fuel
544 Deoxygenation on the Formation of Autoxidative Deposits. *Energy & Fuels*
545 2020;34(11):13814-21.
- 546 [16] Le MD, Matrat M, Amara AB, Foucher F, Moreau B, Yu Y, et al. Antioxidant effect of 2–4
547 xyleneol on fuel oxidation in liquid and gas phase over a wide temperature range. *Fuel*
548 *Processing Technology* 2022;236:107414.
- 549 [17] Zabarnick S, West ZJ, Shafer LM, Mueller SS, Striebich RC, Wrzesinski PJ. Studies of the Role
550 of Heteroatomic Species in Jet Fuel Thermal Stability: Model Fuel Mixtures and Real Fuels.
551 *Energy & Fuels* 2019;33(9):8557-65.
- 552 [18] Alborzi E, Gadsby P, Ismail MS, Sheikhsari A, Dwyer MR, Meijer AJHM, et al. Comparative
553 Study of the Effect of Fuel Deoxygenation and Polar Species Removal on Jet Fuel Surface
554 Deposition. *Energy & Fuels* 2019;33(3):1825-36.
- 555 [19] El-Sayah Z, Glaude P-A, Fournet R, Sirjean B. Comparison of the Effects of Different Biofuels
556 on the Oxidation Stability of a Hydrocarbon Fuel. *SAE Technical Paper* 2020; 2020-01-2101.
- 557 [20] Longanesi L, Pereira AP, Johnston N, Chuck CJ. Oxidative stability of biodiesel: recent insights.
558 *Biofuels, Bioproducts and Biorefining* 2022;16(1):265-89.
- 559 [21] Pullen J, Saeed K. An overview of biodiesel oxidation stability. *Renewable and Sustainable*
560 *Energy Reviews* 2012;16(8):5924-50.
- 561 [22] Yaakob Z, Narayanan BN, Padikkaparambil S, Unni K S, Akbar P M. A review on the oxidation
562 stability of biodiesel. *Renewable and Sustainable Energy Reviews* 2014;35:136-53.
- 563 [23] Bacha K, Ben-Amara A, Vannier A, Alves-Fortunato M, Nardin M. Oxidation Stability of
564 Diesel/Biodiesel Fuels Measured by a PetroOxy Device and Characterization of Oxidation
565 Products. *Energy & Fuels* 2015;29(7):4345-55.
- 566 [24] Ben Amara A, Nicolle A, Alves-Fortunato M, Jeuland N. Toward Predictive Modeling of
567 Petroleum and Biobased Fuel Stability: Kinetics of Methyl Oleate/n-Dodecane Autoxidation.
568 *Energy & Fuels* 2013;27(10):6125-33.
- 569 [25] Di Tommaso S, Rotureau P, Sirjean B, Fournet R, Benaissa W, Gruez P, et al. A mechanistic
570 and experimental study on the diethyl ether oxidation. *Process Safety Progress*
571 2014;33(1):64-9.

- 572 [26] Di Tommaso S, Rotureau P, Benaissa W, Gruez P, Adamo C. Theoretical and Experimental
573 Study on the Inhibition of Diethyl Ether Oxidation. *Energy & Fuels* 2014;28(4):2821-9.
- 574 [27] Jęczmionek Ł, Danek B, Pałuchowska M, Krasodowski W. Changes in the Quality of E15–E25
575 Gasoline during Short-Term Storage up to Four Months. *Energy & Fuels* 2017;31(1):504-13.
- 576 [28] D'Ornellas CV. The Effect of Ethanol on Gasoline Oxidation Stability. *SAE Transactions*
577 2001;110:1963-8.
- 578 [29] Pradelle F, Braga SL, Martins ARFA, Turkovics F, Pradelle RNC. Gum Formation in Gasoline
579 and Its Blends: A Review. *Energy & Fuels* 2015;29(12):7753-70.
- 580 [30] Alves-Fortunato M, Baroni A, Neocel L, Chardin M, Matrat M, Boucaud C, et al. Gasoline
581 Oxidation Stability: Deposit Formation Tendencies Evaluated by PetroOxy and Autoclave
582 Methods and GDI/PFI Engine Tests. *Energy & Fuels* 2021;35(22):18430-40.
- 583 [31] Auzani AS, Clements AG, Hughes KJ, Ingham DB, Pourkashanian M. Assessment of ethanol
584 autoxidation as a drop-in kerosene and surrogates blend with a new modelling approach.
585 *Heliyon* 2021;7(6):e07295.
- 586 [32] Le MD, Warth V, Giarracca L, Moine E, Bounaceur R, Privat R, et al. Development of a
587 Detailed Kinetic Model for the Oxidation of n-Butane in the Liquid Phase. *The Journal of*
588 *Physical Chemistry B* 2021;125(25):6955-67.
- 589 [33] Roohi H, Rajabi M. Iodometric Determination of Hydroperoxides in Hydrocarbon
590 Autoxidation Reactions Using Triphenylphosphine Solution as a Titrant: A New Protocol.
591 *Industrial & Engineering Chemistry Research* 2018;57(20):6805-14.
- 592 [34] Le MD, El Sayah Z, Benrabah R, Warth V, Glaude PA, Privat R, et al. An experimental and
593 detailed kinetic modeling of the thermal oxidation stability of n-decane as a jet fuel surrogate
594 component. *Fuel* 2023;342:127754.
- 595 [35] Kee RJ, Rupley FM, Miller JA. Chemkin-II: A Fortran chemical kinetics package for the analysis
596 of gas-phase chemical kinetics. Sandia National Lab.(SNL-CA), Livermore, CA (United States);
597 1989.
- 598 [36] Baudouin O, Dechelotte S, Guittard P, Vacher A. Simulis® Thermodynamics: an open
599 framework for users and developers. In: Braunschweig B, Joulia X, editors. *Computer Aided*
600 *Chemical Engineering*. Elsevier; 2008, p. 635-40.
- 601 [37] Frisch MJ, Trucks GW, Schlegel HB, Scuseria GE, Robb MA, Cheeseman JR, et al. *Gaussian 16*
602 *Rev. C.01*. Wallingford, CT; 2016.
- 603 [38] Lizardo-Huerta JC, Sirjean B, Verdier L, Fournet R, Glaude PA. The decisive role of pericyclic
604 reactions in the thermal decomposition of organophosphorus compounds. *Proceedings of*
605 *the Combustion Institute* 2021;38(1):719-27.
- 606 [39] Goldsmith CF, Magoon GR, Green WH. Database of Small Molecule Thermochemistry for
607 Combustion. *The Journal of Physical Chemistry A* 2012;116(36):9033-57.
- 608 [40] Klamt A, Eckert F. COSMO-RS: a novel and efficient method for the a priori prediction of
609 thermophysical data of liquids. *Fluid Phase Equilibria* 2000;172(1):43-72.
- 610 [41] Steffen C, Thomas K, Huniar U, Hellweg A, Rubner O, Schroer A. TmoleX—A graphical user
611 interface for TURBOMOLE. *Journal of Computational Chemistry* 2010;31(16):2967-70.
- 612 [42] Oyeyemi VB, Keith JA, Carter EA. Trends in Bond Dissociation Energies of Alcohols and
613 Aldehydes Computed with Multireference Averaged Coupled-Pair Functional Theory. *The*
614 *Journal of Physical Chemistry A* 2014;118(17):3039-50.
- 615 [43] Luo Y-R. *Handbook of bond dissociation energies in organic compounds*. Boca Raton: CRC
616 Press; 2002.
- 617 [44] Moine E, Privat R, Sirjean B, Jaubert J-N. Estimation of solvation quantities from experimental
618 thermodynamic data: Development of the comprehensive CompSol databank for pure and
619 mixed solutes. *Journal of Physical and Chemical Reference Data* 2017;46(3):033102.

620